Chapter 5
Estimation of Road Profile and External Forces as Unknown Inputs

Abstract. This chapter is devoted to the application of sliding mode observers to estimate the unknown inputs of the road. Vehicle motion simulation accuracy, such as in accident reconstruction or vehicle controllability analysis on real roads, can be obtained only if valid road profile and tire-road friction models are available. Regarding road profiles, a new method based on Sliding Mode Observers has been developed and is compared to two inertial methods. Experimental results are shown and discussed to evaluate the robustness and the quality of the proposed approach.

5.1 Introduction

Road profile unevenness through road/vehicle dynamic interaction and vehicle vibration affects safety (tyre contact forces), ride comfort, energy consumption and wear. The road profile unevenness is consequently a basic information for road maintenance management systems [VP91]. In order to obtain this road profile, several methods have been developed. Measurement of road roughness has been a subject of numerous research for more than 70 years ([Har83], [MW86], [Mis90]). Methods developed can be classified into two types: response type and profiling method. Nowadays profiling methods giving a road profile along a measuring line are generally preferred. These methods belong to two basic techniques: rolling beam or inertial profiling method. The last method, which was first proposed in 1964 [SK64], is now used worldwide. Inertial profiling methods consist in analyzing the signal coming from displacement sensors and accelerometers ([Kar84], [GSH87]). One problem with the inertial profiling method, as currently used, is that it is impossible to build a $3D$ profile from elementary measurements needed for road/vehicle interaction simulation package. It is worthwhile mentioning that these methods do not take into consideration the dynamic behavior of the vehicle. However, it has been shown that modifications of the dynamic behavior may lead to biased results.

H. Imine et al.: Sliding Mode Based Analysis, LNCIS 414, pp. 83–102.
springerlink.com

Finding a way to get a $3D$ profile from the dynamic response of an instrumented car driven on a chosen road section is the general purpose of a research carried out at Roads and Bridges Central Laboratory (in French: LCPC) in cooperation with the Robotics Laboratory of Versailles (in French: LRV) [Imi03].

The proposed method estimates the unknown inputs of the system corresponding to the height of the road through the use of sliding mode observers ([BZ88], [XG88], [Dra92], [BBD96], [DBB99], [DB02]).

Design of such observers requires a dynamic model. As a first step, a dynamic model of a vehicle is built up ([Men97], [Imi03]). This model has been experimentally validated comparing the estimated and measured dynamics in the response of a Peugeot 406 vehicle (as a test car). The longitudinal forces which depend on the road adhesion coefficients are estimated using a sliding mode observer (see [Can98], [IDM03]).

The second section of this chapter deals with the vehicle description and modeling. Then the observer design is presented in the third section in order to estimate the unknown inputs. Some simulation and experimental results are given in this section. The estimation of unknown forces is presented in the section four and a second approach to estimate the unknown inputs is presented. The main experimental results are presented in order to show the accuracy of the estimated road profile coming from the observer based method. Finally, the last section concludes on the effectiveness of the presented methods.

5.2 Vehicle Modeling

In this section, we are interested in the excitations of pavement and the vehicle/road interaction. The model is established while making the following simplifying hypotheses:

- The vehicle is rolling with a constant speed.
- The wheels are rolling without slip and without contact loss.

The vertical motion of the vehicle model can be described by the following equation:

$$M\ \ddot{q} + C\ \dot{q} + Kq = AU + \Omega, \tag{5.1}$$

where $q = \left[\, z_1\ z_2\ z_3\ z_4\ z\ \theta\ \phi\ \psi \,\right]^T$ is the coordinates vector , $\dot{q}$ represent the velocities vector and $\ddot{q}$ the accelerations vector.

The vector $U = \left[\, u_1\ u_2\ u_3\ u_4\ \dot{u}_1\ \dot{u}_2\ \dot{u}_3\ \dot{u}_4 \,\right]^T$ is the road inputs vector.

The vector $\Omega = [0\ 0\ 0\ 0\ 0\ 0\ 0\ f(\delta_f, \beta)]^T$ is a function of the steering angle δ_f and the side slip angle β. The function $f(\delta_f, \beta)$ is given by:

$$f(\delta_f, \beta) = -2(r_1 C_{yf} - r_2 C_{yr})\beta + 2r_1 C_{yf}\delta_f. \tag{5.2}$$

$M \in \mathbb{R}^{8\times 8}$ represent the mass matrix:

$$M = \begin{bmatrix} m_1 & 0 & 0 & 0 & 0 & 0 & 0 & 0 \\ 0 & m_2 & 0 & 0 & 0 & 0 & 0 & 0 \\ 0 & 0 & m_3 & 0 & 0 & 0 & 0 & 0 \\ 0 & 0 & 0 & m_4 & 0 & 0 & 0 & 0 \\ 0 & 0 & 0 & 0 & m & 0 & 0 & 0 \\ 0 & 0 & 0 & 0 & 0 & J_{xx} & 0 & 0 \\ 0 & 0 & 0 & 0 & 0 & 0 & J_{yy} & 0 \\ 0 & 0 & 0 & 0 & 0 & 0 & 0 & J_{zz} \end{bmatrix}. \tag{5.3}$$

where m_i is the mass of the wheel i, m is the spring mass, J_{xx}, J_{yy} and J_{zz} are respectively the moments of inertia along X, Y and Z axis.

$C \in \mathbb{R}^{8\times 8}$ is the damping matrix:

$$C = \begin{bmatrix} (B_1 + B_{r1}) & 0 & 0 & 0 & -B_1 & C_{16} & C_{17} & 0 \\ 0 & (B_2 + B_{r2}) & 0 & 0 & -B_2 & C_{26} & C_{27} & 0 \\ 0 & 0 & (B_3 + B_{f1}) & 0 & -B_3 & C_{36} & C_{37} & 0 \\ 0 & 0 & 0 & (B_4 + B_{f2}) & -B_4 & C_{46} & C_{47} & 0 \\ -B_1 & -B_2 & -B_3 & -B_4 & C_{55} & C_{56} & C_{57} & 0 \\ B_1 p_r & -B_2 p_r & B_3 p_f & -B_4 p_f & C_{65} & C_{66} & C_{67} & 0 \\ B_1 r_2 & B_2 r_2 & -B_3 r_1 & -B_4 r_1 & C_{75} & C_{76} & C_{77} & 0 \\ C_{81} & C_{82} & C_{83} & C_{84} & C_{85} & C_{86} & C_{87} & C_{88} \end{bmatrix} \tag{5.4}$$

The matrix $K \in \mathbb{R}^{8\times 8}$ is function of spring coefficients:

$$K = \begin{bmatrix} k_1 + k_{r1} & 0 & 0 & 0 & -k_1 & k_1 p_r & k_1 r_2 & 0 \\ 0 & k_2 + k_{r2} & 0 & 0 & -k_2 & -k_2 p_r & k_2 r_2 & 0 \\ 0 & 0 & k_3 + k_{f1} & 0 & -k_3 & k_3 p_f & -k_3 r_1 & 0 \\ 0 & 0 & 0 & k_4 + k_{f2} & -k_4 & -k_4 p_f & -k_4 r_1 & 0 \\ -k_1 & -k_2 & -k_3 & -k_4 & K_{55} & K_{56} & K_{57} & 0 \\ k_1 p_r & -k_2 p_r & k_3 p_f & -k_4 p_f & K_{65} & K_{66} & K_{67} & 0 \\ k_1 r_2 & k_2 r_2 & -k_3 r_1 & -k_4 r_1 & K_{75} & K_{76} & K_{77} & 0 \\ K_{81} & K_{82} & K_{83} & K_{84} & K_{85} & K_{86} & K_{87} & K_{88} \end{bmatrix}. \tag{5.5}$$

The matrix $A \in \mathbb{R}^{8\times 8}$ is composed of spring and damping coefficients:

$$A = \begin{bmatrix} k_{r1} & 0 & 0 & 0 & B_{r1} & 0 & 0 & 0 \\ 0 & k_{r2} & 0 & 0 & 0 & B_{r2} & 0 & 0 \\ 0 & 0 & k_{f1} & 0 & 0 & 0 & B_{f1} & 0 \\ 0 & 0 & 0 & k_{f2} & 0 & 0 & 0 & B_{f2} \\ 0 & 0 & 0 & 0 & 0 & 0 & 0 & 0 \\ 0 & 0 & 0 & 0 & 0 & 0 & 0 & 0 \\ 0 & 0 & 0 & 0 & 0 & 0 & 0 & 0 \\ 0 & 0 & 0 & 0 & 0 & 0 & 0 & 0 \end{bmatrix} . \tag{5.6}$$

We then rewrite the model in the state form as (5.1) :

$$\begin{cases} x_1 = q \\ \dot{x}_1 = x_2 \\ \dot{x}_2 = \ddot{x}_1 = \ddot{q} = M^{-1}(-Cx_2 - Kx_1 + Ax_3 + \Omega) \\ \dot{x}_3 = x_4 = \dot{U} \\ y = x_1 \end{cases} . \tag{5.7}$$

where y is the output vector:

$$y = \left[z_1 \; z_2 \; z_3 \; z_4 \; z \; \theta \; \phi \; \psi \right]^T . \tag{5.8}$$

In the following section, a sliding mode observer is developed in order to estimate the unknown inputs of the system.

5.3 Sliding Mode Observer and Estimation of Unknown Inputs

The construction of the observer is done using 3 steps as we explain in this section. After that, we present and we discuss some simulation results.

5.3.1 Observability Study

In order to study the observability of the system (5.1), let us define the functions f and h as:

$$\begin{cases} f(x, U) = M^{-1}(-Cx_2 - Kx_1 + AU + \Omega) \\ y = h(x) \end{cases} . \tag{5.9}$$

where $x = (x_1, x_2)^T$ is a vector of dimension n.

The system is considered to be observable if the matrix MO defined below is of rank n (see [Bou97]) (in our case $n = 16$):

$$MO = \begin{bmatrix} dh(x) \\ dL_f h(x) \\ \vdots \\ \vdots \\ dLf\ ^{15}h(x) \end{bmatrix}. \tag{5.10}$$

where $dh = (\frac{\partial h}{\partial x_1}, \frac{\partial h}{\partial x_2}, ..., \frac{\partial h}{\partial x_{16}})$ and $L_f(h)(x) = \sum_{i=1}^{16} f_i \frac{\partial h}{\partial x_i}$.

The calculation of this matrix using Matlab shows that the rank of MO is 16. We deduce that the system (5.1) is observable.

5.3.2 Observer Design

This section is devoted to sliding mode observer design in order to estimate the vectors $\dot{q}$ and $\ddot{q}$ and to then reconstruct the unknown inputs vector U ([SHM86], [ILMD02a]).

Before developing the observer, we notice that the system satisfies the following hypothesis:

a) The state of the system is bounded ($\| x(t) \| < \infty \ \forall\ t \geq 0$). The vehicle states are bounded.

b) The system is input bounded (for $i = 1..4$ a constant $\mu_i \in \mathbb{R}$ $existssuchthat \|\dot{u}_i\| < \mu_i$);

c) The amplitude of the inputs representing the road are very low and not greater than $10^{-3}m$. We can then assume that their accelerations are small and neglected $\ddot{x}_3 = \dot{x}_4 = \ddot{U} = 0$.

Assuming that the dynamic parameters of the vehicle are well known, we can write the observer as:

$$\begin{cases} \dot{\hat{x}}_1 = \hat{x}_2 + H_1 sign(\tilde{x}_1) \\ \dot{\hat{x}}_2 = M^{-1}(-C\hat{x}_2 - K\hat{x}_1 + A\hat{x}_3 + \Omega) + H_2 sign(\tilde{x}_1)\ . \\ \dot{\hat{x}}_3 = \hat{x}_4 + H_3 sign(\tilde{x}_1) \end{cases} \tag{5.11}$$

where $\hat{x}_i$ represents the observed state vector of x_i.

$H_i \in \mathbb{R}^{8\times 8}$, $i = 1, 2$, are diagonal positive gains matrices and the "$sign$" are defined as follows:

$$\left.\begin{cases} H_1 = diag\{H_{1_1}, H_{1_2}, H_{1_3}, H_{1_4}, H_{1_5}, H_{1_6}, H_{1_7}, H_{1_8}\} \\ H_2 = diag\{H_{2_1}, H_{2_2}, H_{2_3}, H_{2_4}, H_{2_5}, H_{2_6}, H_{2_7}, H_{2_8}\} \\ sign(\tilde{x}_1) = diag\{\tilde{x}_{1_1}, \tilde{x}_{1_2}, \tilde{x}_{1_3}, \tilde{x}_{1_4}, \tilde{x}_{1_5}, \tilde{x}_{1_6}, \tilde{x}_{1_7}, \tilde{x}_{1_8}\}^T \end{cases}\right| \tag{5.12}$$

The matrix $H_3 \in \mathbb{R}^{8\times 8}$ is to be defined during the convergence study.

The estimation error of the variable x_i is obtained by:

$$\tilde{x}_i = x_i - \hat{x}_i, \quad i = 1..3. \tag{5.13}$$

The dynamic error of the observer is obtained through the difference between systems (5.7) and (5.11) as following:

$$\begin{cases} \dot{\tilde{x}}_1 = \tilde{x}_2 - H_1 sign(\tilde{x}_1) \\ \dot{\tilde{x}}_2 = -M^{-1}(C\ \tilde{x}_2 + K\ \tilde{x}_1) + M^{-1}A\ \tilde{x}_3 - H_2 sign(\tilde{x}_1)\ . \\ \dot{\tilde{x}}_3 = \tilde{x}_4 - H_3 sign(\tilde{x}_1) \end{cases} \tag{5.14}$$

5.3.3 Convergence Study

As we showed previously, and in order to study the convergence of the observer, we proceed step by step. We first prove the convergence of the position ($\tilde{x}_1 = 0$). We must prove that the sliding surface is attractive ($\tilde{x}_1 = 0$). Then, we will study the convergence of the speed $\tilde{x}_2$. At this moment, we can deduce that the estimation error of the input ($\tilde{x}_3$) converges towards 0.

5.3.3.1 Convergence of the Position

Let us consider the following Lyapunov function:

$$V_1 = \frac{1}{2}\tilde{x}_1^T \tilde{x}_1, \tag{5.15}$$

Its derivative gives:

$$\dot{V}_1 = \tilde{x}_1^T \dot{\tilde{x}}_1, \tag{5.16}$$

From (5.14), we obtain:

$$\dot{V}_1 = \tilde{x}_1^T (\tilde{x}_2 - H_1 sign(\tilde{x}_1)). \tag{5.17}$$

Choosing the gain matrices $H_1 = diag(h_{i1})$, as $h_{i1} > |\tilde{x}_{i2}|$ for $i = 1...8$, we prove that $\dot{V}_1 < 0$. Then, $\hat{x}_1$ converges towards x_1 in finite time t_0. In this case, $\dot{\tilde{x}}_1 = 0\ \forall\ t > t_0$.

This implies, from relationship (5.17), that we obtain:

$$sign_{eq}(\tilde{x}_1) = H_1^{-1}\tilde{x}_2 \qquad , \tag{5.18}$$

where $sign_{eq}$ is the equivalent mean of the $sign$ function in the sliding surface:

Taking into account (5.18) and since $\tilde{x}_4$ is bounded, then equations (5.14) become:

$$\begin{cases} \dot{\tilde{x}}_1 = \tilde{x}_2 - H_1 sign(\tilde{x}_1) \to 0 \\ \dot{\tilde{x}}_2 = -M^{-1}C\ \tilde{x}_2 + M^{-1}A\ \tilde{x}_3 - H_2 H_1^{-1}\tilde{x}_2\ . \\ \dot{\tilde{x}}_3 = -H_3 H_1^{-1}\tilde{x}_2 \end{cases} \tag{5.19}$$

5.3.3.2 Speed Convergence

Consider now a following second Lyapunov function:

$$V_2 = \frac{1}{2}\tilde{x}_2^T M \tilde{x}_2 + \frac{1}{2}\tilde{x}_3^T P_1 \tilde{x}_3, \tag{5.20}$$

where $P_1 \in \mathbb{R}^{8\times 8}$ is a diagonal positive matrix:

The calculation of $\dot{V}_2$ gives, using the equations (5.19),:

$$\dot{V}_2 = -\tilde{x}_2^T C \tilde{x}_2 - \tilde{x}_2^T M H_2 H_1^{-1} \tilde{x}_2 + \tilde{x}_2^T A \tilde{x}_3 - \tilde{x}_3^T P_1 H_3 H_1^{-1} \tilde{x}_2. \tag{5.21}$$

Choosing the gains ($P_1 = diag(P_{1i})$, $i = 1..8$) such as $A^T = P_1 H_3 H_1^{-1}$, the matrix H_3 is deduced as follows:

$$H_3 = P_1^{-1} A^T H_1. \tag{5.22}$$

Replacing the matrices P_1, A^T and H_1 by their respective values, we obtain the elements of the matrix H_3 :

$$H_3 == \begin{bmatrix} H_{11}k_{r1}/P_{11} & 0 & 0 & 0 & 0\ 0\ 0\ 0 \\ 0 & H_{22}k_{r2}/P_{22} & 0 & 0 & 0\ 0\ 0\ 0 \\ 0 & 0 & H_{33}k_{f1}/P_{33} & 0 & 0\ 0\ 0\ 0 \\ 0 & 0 & 0 & H_{44}k_{f2}/P_{44} & 0\ 0\ 0\ 0 \\ H_{11}B_{r1}/P_{55} & 0 & 0 & 0 & 0\ 0\ 0\ 0 \\ 0 & H_{22}B_{r2}/P_{66} & 0 & 0 & 0\ 0\ 0\ 0 \\ 0 & 0 & H_{33}B_{f1}/P_{77} & 0 & 0\ 0\ 0\ 0 \\ 0 & 0 & 0 & H_{44}B_{f2}/P_{88} & 0\ 0\ 0\ 0 \end{bmatrix}. \tag{5.23}$$

$\dot{V}_2$ becomes:

$$\dot{V}_2 = -\tilde{x}_2^T (C + M H_2 H_1^{-1}) \tilde{x}_2. \tag{5.24}$$

We defined a matrix Q as:

$$Q = C + M H_2 H_1^{-1}. \tag{5.25}$$

The gains of matrix H_2 are chosen in order to satisfy that matrix Q be definite positive . In this case, we have $\dot{V}_2 < 0$ and the observation error is decreasing, which implies that the condition $h_{i1} > |\tilde{x}_{i2}|$ is always verified for $t > t_0$. The surface $\tilde{x}_2 = 0$ is then attractive and thus means that $\hat{x}_2$ converges asymptotically toward x_2.

Equations (5.19) allow deducing that the estimation errors of the derivative of the road profile tend towards 0.

5.3.4 Estimation Results

In order to validate the proposed approach, some simulation experimental results are given.

5.3.4.1 Simulation Results

In this section we give some simulation results obtained using sliding mode observers. These observers make it possible to reconstruct the states of the system, and thus to consider the unknown inputs of the road. It is assumed that the deflection of the chassis and the four wheels and also the rotation of the chassis (roll, pitch and yaw angle) are measured by sensors. That being said, several other signals are assumed to be known, such as the vehicle speed and steering angle.

The main estimate is shown in Fig. 5.1.

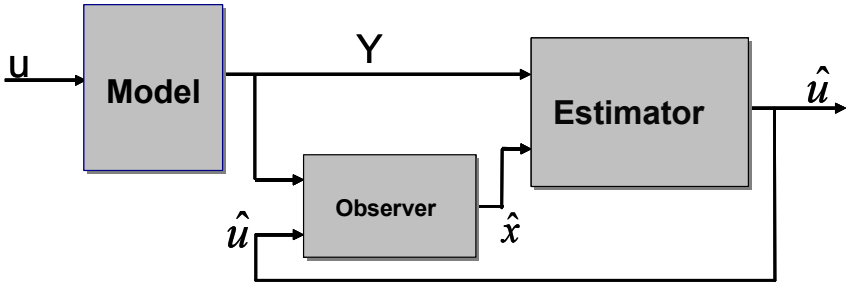

Fig. 5.1 Estimation principle

The input signals used in this simulation are those measured by Selcom sensors during tests done at LCPC with an instrumented *Peugeot* 406 rolling at a constant speed of about $72km/h$.

The estimated vertical displacement of the chassis (z) and the estimated roll angle (θ) and their equivalent measurements are represented in Fig. 5.2.

These figures show the accurate estimation of the displacement and also of the roll angle since the correlation of the figures is clearly shown.

The other figures of the second line represent, respectively, the vertical speed of the chassis and the roll rate. One can notice that the estimates follow closely the speeds given by the model.

However, a small variation exists on the estimated roll rate. The estimation of the road profile is given in Fig. 5.3 and Fig. 5.4 which represent, respectively, the right and the left road profile compared to the LPA measurements.

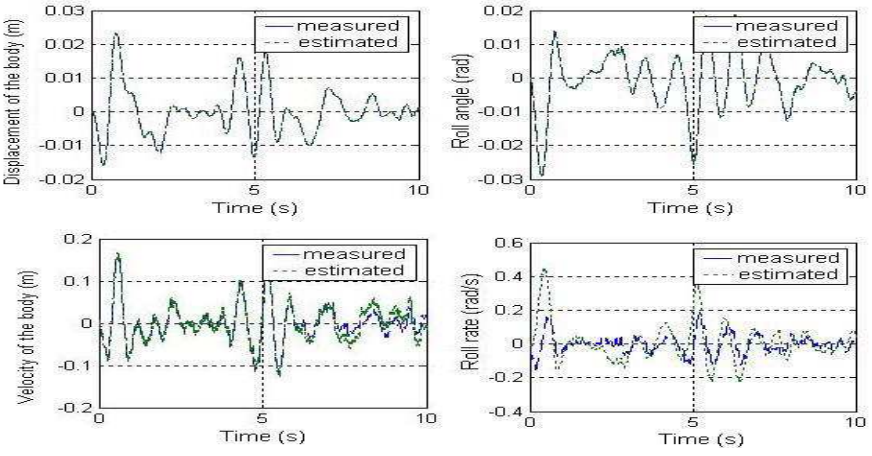

Fig. 5.2 Vehicle states estimation: roll angle and displacement of the chassis

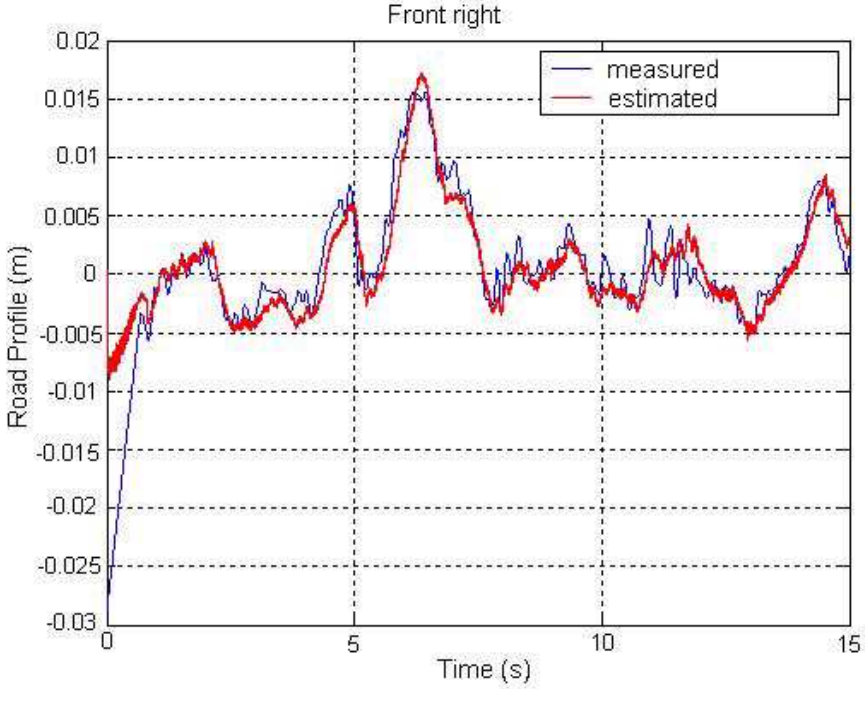

Fig. 5.3 Road profile estimation: front right

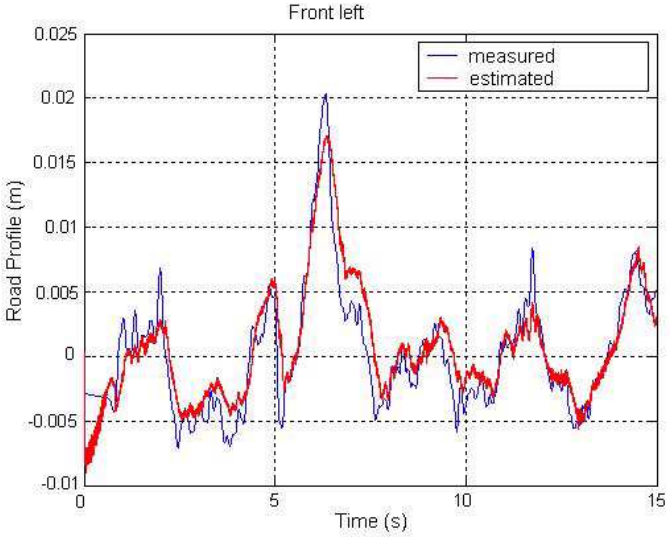

Fig. 5.4 Road profile estimation: front left

One can remark from these figures that the estimated road profile is correct compared to those measured by APL.

5.3.4.2 Experimental Results

In this part, the measured signals coming from sensors are compared to those estimated by the observer.

The estimation principle is shown in Fig. 5.5.

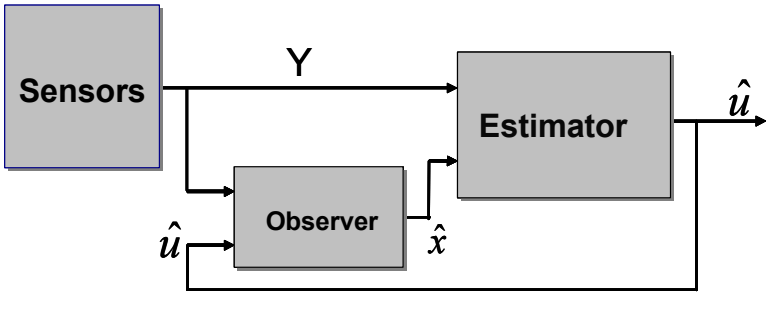

Fig. 5.5 Estimation principle

The following gains are used: $P_1 = diag(100, 100, 100, 100, 100, 100, 100, 100)$, $H_1 = diag(1, 1, 1, 1, 1, 1, 1, 1)$, the elements of matrix H_3 are given by: $H_3(1,1) = 1000$, $H_3(2,2) = 1000$, $H_3(3,3) = 1000$, $H_3(4,4) = 1000$, $H_3(5,1) = 5$, $H_3(6,2) = 5$, $H_3(7,3) = 5$, $H_3(8,4) = 5$.

The vertical displacement and the yaw angle are shown in Fig. 5.6.

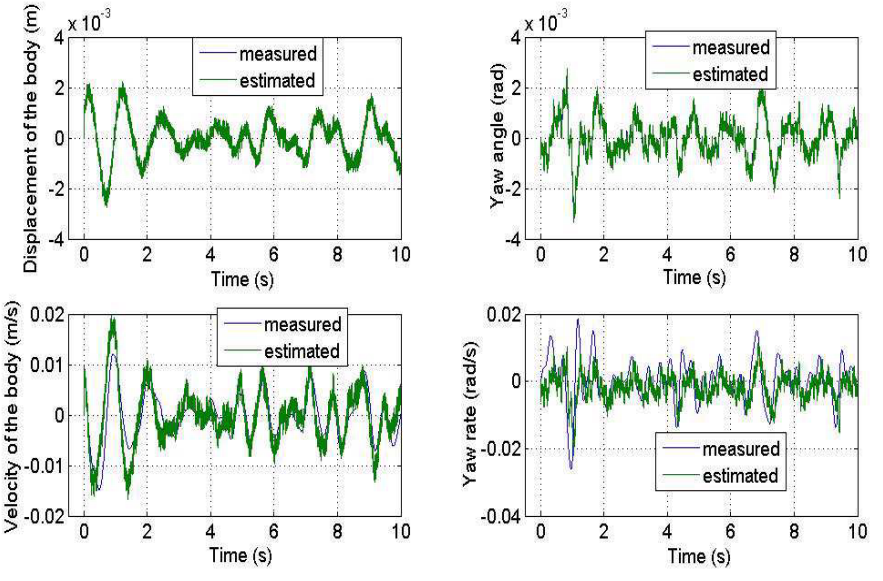

Fig. 5.6 States estimation: experimental case

The convergence is quick and in finite time. In the second line, the equivalent speeds are represented.

A well estimation of the vertical speed can be noticed. However some chattering exist concerning the estimated yaw rate. This is due to sensor errors.

In Fig. 5.7 the estimated road profile is shown.

This figures shows that the unknown input is well estimated compared to LPA measure with some chattering due to the *sign* function used in the observer.

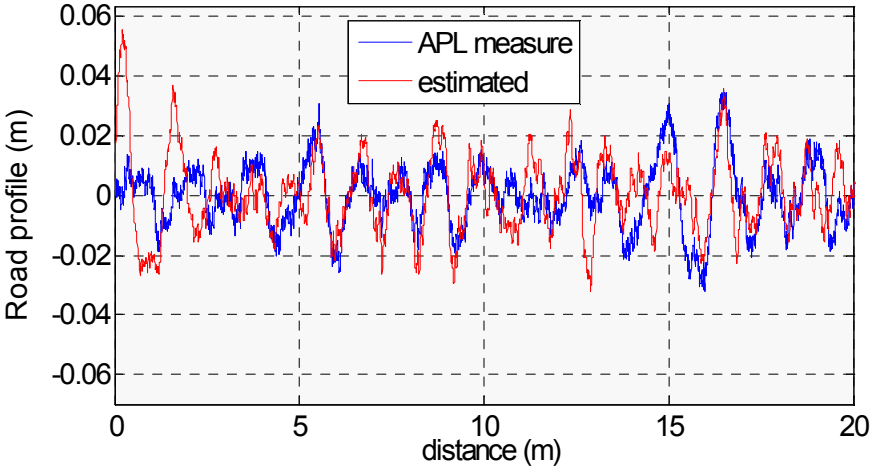

Fig. 5.7 Road profile estimation: experimental case

5.4 Unknown Forces Estimation

The parameters used in our vehicle model are considered constant and measured. However, some parameters depend on the type and the quality of the road and are generally not well known.

Coefficients intervening in the calculation of the adhesion are included in this category. Our idea consists in considering the longitudinal forces of the wheels which are a function of the road adhesion coefficient jointly as unknown states ([HI01], [MT99], [HCB+01], [HCM01], [HCBM02], [IMD03], [IDM03]).

In our case, four measurements of the speeds of the wheels are added to the previously measured vector.

The vector y becomes:

$$y = \left[z_1 \; z_2 \; z_3 \; z_4 \; z \; \theta \; \phi \; \psi \; w_{r1} \; w_{r2} \; w_{f1} \; w_{f2} \right]^T \tag{5.26}$$

Before developing the observer, let us define the new state vector $x = [x_1, x_2, x_3, x_4]^T$ as follows:

$$\begin{cases} x_1 = \left[z_1 \; z_2 \; z_3 \; z_4 \; z \; \theta \; \phi \; \psi \right]^T \\ x_2 = \left[\dot{z}_1 \; \dot{z}_2 \; \dot{z}_3 \; \dot{z}_4 \; \dot{z} \; \dot{\theta} \; \dot{\phi} \; \dot{\psi} \; w_{r1} \; w_{r2} \; w_{f1} \; w_{f2} \right]^T \\ x_3 = U = \left[u_1 \; u_2 \; u_3 \; u_4 \; \dot{u}_1 \; \dot{u}_2 \; \dot{u}_3 \; \dot{u}_4 \right]^T \\ x_4 = \dot{x}_3 \end{cases} \tag{5.27}$$

where

$$\begin{cases} \dot{x}_1 = \Lambda_1 = [\dot{z}_1 \; \dot{z}_2 \; \dot{z}_3 \; \dot{z}_4 \; \dot{z} \; \dot{\theta} \; \dot{\phi} \; \dot{\psi}]^T = E_1 x_2 \\ \dot{\Lambda}_1 = M^{-1}(-C\Lambda_1 - Kx_1 + Ax_3 + \Omega) \end{cases} \tag{5.28}$$

$E_1 \in \mathbb{R}^{8\times 12}$ is a definite positive matrix such that its elements $E_{ij} \in \{0, 1\}$.

The rotational movement of the wheels are given by:

$$\dot{\Lambda}_2 = J^{-1}(\Gamma + R\Psi), \tag{5.29}$$

where $\Lambda_2 = \begin{bmatrix} w_{r1} \; w_{r2} \; w_{f1} \; w_{f2} \end{bmatrix}^T = E_2 x_2$ is the vector of wheel speeds, $E_2 \in \mathbb{R}^{4\times 12}$ is a positive matrix where its elements E_{ij} are defined in the domain $\{0, 1\}$. $\Psi = [F_{xr1}, F_{xr2}, F_{xf1}, F_{xf2}]^T$ represent the longitudinal vector forces. We assume that the derivative of these forces are neglected ($\dot{\Psi} = 0$).

J is a diagonal matrix composed of the inertia of the wheels:

$$J = \begin{bmatrix} J_r & 0 & 0 & 0 \\ 0 & J_r & 0 & 0 \\ 0 & 0 & J_f & 0 \\ 0 & 0 & 0 & J_f \end{bmatrix}, \tag{5.30}$$

where Γ is matrix composed of the engine torquesM_{f1}, M_{f2} :

$$\Gamma = \begin{bmatrix} 0 & 0 & 0 & 0 \\ 0 & 0 & 0 & 0 \\ 0 & 0 & M_{f1} & 0 \\ 0 & 0 & 0 & M_{f2} \end{bmatrix}, \tag{5.31}$$

with $R = r* I$ where r is the wheel radius and $I \in \mathbb{R}^{4\times 4}$ is identity matrix:

The variable state $\dot{x}_2$ is then given by:

$$\dot{x}_2 = A_1\dot{\Lambda}_1 + A_2\dot{\Lambda}_2. \tag{5.32}$$

The matrices $A_1 \in \mathbb{R}^{12\times 8}$ and $A_2 \in \mathbb{R}^{12\times 4}$ are defined in the Appendix.

The proposed observer is:

$$\begin{cases} \dot{\hat{x}}_1 = \hat{\Lambda}_1 + H_1 sign(\tilde{x}_1) \\ \dot{\hat{\Lambda}}_1 = M^{-1}(-C\ \hat{\Lambda}_1 - K\ \hat{x}_1 + A\ \hat{x}_3 + \Omega) + H_2 sign(\tilde{x}_1) \\ \dot{\hat{\Lambda}}_2 = J^{-1}\Gamma + J^{-1}R\ \hat{\Psi} \\ \dot{\hat{x}}_3 = \hat{x}_4 + H_3 sign(\tilde{x}_1) \\ \dot{\hat{\Psi}} = \mu \end{cases}. \tag{5.33}$$

where μ is an adaptation term to be defined. $H_i \in \mathbb{R}^{8\times 8}$, $i = 1..3$ are diagonal positive gains matrices and the "$sign$", defined as follows:

$$\left.\begin{cases} H_1 = diag\{H_{1_1}, H_{1_2}, H_{1_3}, H_{1_4}, H_{1_5}, H_{1_6}, H_{1_7}, H_{1_8}\} \\ H_2 = diag\{H_{2_1}, H_{2_2}, H_{2_3}, H_{2_4}, H_{2_5}, H_{2_6}, H_{2_7}, H_{2_8}\} \\ H_3 = diag\{H_{3_1}, H_{3_2}, H_{3_3}, H_{3_4}, H_{3_5}, H_{3_6}, H_{3_7}, H_{3_8}\} \\ sign(\tilde{x}_1) = diag\{\tilde{x}_{1_1}, \tilde{x}_{1_2}, \tilde{x}_{1_3}, \tilde{x}_{1_4}, \tilde{x}_{1_5}, \tilde{x}_{1_6}, \tilde{x}_{1_7}, \tilde{x}_{1_8}\}^T \end{cases}\right| \tag{5.34}$$

The variable $\tilde{x}_i = x_i - \hat{x}_i, \quad i = 1..4$ represents the estimation error of x_i, $\tilde{\Lambda}_i = \Lambda_i - \hat{\Lambda}_i$ is the estimation error of $\Lambda_i (i = 1..2)$. $\tilde{\Psi} = \Psi - \hat{\Psi}$ is the estimation error of longitudinal forces.

The dynamic observation error is given by:

$$\begin{cases} \dot{\tilde{x}}_1 = \tilde{\Lambda}_1 - H_1 sign(\tilde{x}_1) \\ \dot{\tilde{\Lambda}}_1 = M^{-1}(-C\ \tilde{\Lambda}_1 - K\ \tilde{x}_1 + A\ \tilde{x}_3) - H_2 sign(\tilde{x}_1) \\ \dot{\tilde{\Lambda}}_2 = J^{-1} R\ \tilde{\Psi} \\ \dot{\tilde{x}}_3 = \tilde{x}_4 - H_3 sign(\tilde{x}_1) \\ \dot{\tilde{\Psi}} = -\mu \end{cases} . \tag{5.35}$$

5.4.1 Convergence Study

The convergence study of the observer is done step by step. First the convergence of the position x_1 is done.

Let us define the following Lyapunov function:

$$V_1 = \frac{1}{2}\tilde{x}_1^T \tilde{x}_1 \tag{5.36}$$

Its derivative is given by:

$$\dot{V}_1 = \tilde{x}_1^T \dot{\tilde{x}}_1 \tag{5.37}$$

Using (5.35), we obtain:

$$\dot{V}_1 = \tilde{x}_1^T (\tilde{\Lambda}_1 - H_1 sign(\tilde{x}_1)) \tag{5.38}$$

The gain matrix $H_1 = diag(h_{i1})$ is chosen such that $h_{i1} > \left|\tilde{\Lambda}_{i1}\right|$ for $i = 1...8$. We then have $\dot{V}_1 < 0$, which implies that $\hat{x}_1$ tends toward x_1 in finite time t_0. We the obtain $\dot{\tilde{x}}_1 = 0\ \forall\ t > t_0$.

The function $sign_{eq}$ is then defined as the $sign$ function in the sliding surface.

$$sign_{eq}(\tilde{x}_1) = H_1^{-1} \tilde{\Lambda}_1 \tag{5.39}$$

The equation system defined in (5.35) becomes $\forall\ t > t_0$:

$$\begin{cases} \dot{\tilde{x}}_1 = 0 \\ \dot{\tilde{\Lambda}}_1 = M^{-1}(-C\ \tilde{\Lambda}_1 + A\ \tilde{x}_3) - H_2 H_1^{-1} \tilde{\Lambda}_1 \\ \dot{\tilde{\Lambda}}_2 = J^{-1} R\ \tilde{\Psi} \\ \dot{\tilde{x}}_3 = \tilde{x}_4 - H_3 H_1^{-1} \tilde{\Lambda}_1 \\ \dot{\tilde{\Psi}} = -\mu \end{cases} \tag{5.40}$$

In order to prove the convergence of x_2 and then estimate the unknown input vector $\hat{U}$ and the unknown forces vector $\hat{\Psi}$, a second Lyapunov function is considered:

$$V_2=\frac{1}{2}\tilde{\Lambda}_1^T M\tilde{\Lambda}_1+\frac{1}{2}\tilde{\Lambda}_2^T\tilde{\Lambda}_2+\frac{1}{2}\tilde{x}_3^T P_1\tilde{x}_3+\frac{1}{2}\tilde{\Psi}^T P_2\tilde{\Psi} \tag{5.41}$$

where $P_1 \in \mathbb{R}^{8\times 8}$ and $P_2 \in \mathbb{R}^{4\times 4}$ are diagonal positive matrices:

Its derivative gives:

$$\dot{V}_2 = \tilde{\Lambda}_1^T\dot{\tilde{\Lambda}}_1 + \tilde{\Lambda}_2^T\dot{\tilde{\Lambda}}_2 + \tilde{x}_3^T P_1\dot{\tilde{x}}_3 + \tilde{\Psi}^T P_2\dot{\tilde{\Psi}} \tag{5.42}$$

From equation (5.40) and since $\tilde{x}_4$ is bounded, we obtain:

$$\begin{aligned}\dot{V}_2 = &-\tilde{\Lambda}_1^T C\tilde{\Lambda}_1 - \tilde{\Lambda}_1^T M H_2 H_1^{-1}\tilde{\Lambda}_1 + \tilde{\Lambda}_1^T A\tilde{x}_3 \\ &-\tilde{x}_3^T P_1 H_3 H_1^{-1}\tilde{\Lambda}_1 + \tilde{\Lambda}_2^T J^{-1} R\,\tilde{\Psi} - \tilde{\Psi}^T P_2\mu\end{aligned} \tag{5.43}$$

Choosing matrix P_1 such that $A^T = P_1 H_3 H_1^{-1}$, we obtain the gain matrix H_3 as:

$$H_3 = P_1^{-1} A^T H_1 \tag{5.44}$$

The function $\dot{V}_2$ becomes:

$$\dot{V}_2 = -\tilde{\Lambda}_1^T C\tilde{\Lambda}_1 - \tilde{\Lambda}_1^T M H_2 H_1^{-1}\tilde{\Lambda}_1 + \tilde{\Lambda}_2^T J^{-1} R\,\tilde{\Psi} - \tilde{\Psi}^T P_2\mu \tag{5.45}$$

The adaptive term μ is then deduced as follows:

$$\begin{aligned}\mu &= P_2^{-1}(J^{-1}R)^T\tilde{\Lambda}_2^T \\ &= P_2^{-1}\Omega^T\tilde{\Lambda}_2^T\end{aligned} \tag{5.46}$$

where $\Omega = J^{-1}R$.

We finally obtain:

$$\dot{V}_2 = -\tilde{\Lambda}_1^T(C + M H_2 H_1^{-1})\tilde{\Lambda}_1 \tag{5.47}$$

The gain matrix H_2 is chosen such that the matrix $Q_1 = C + M H_2 H_1^{-1}$ is definite positive. Consequently, $\dot{V}_2 < 0$, which implies the asymptotic convergence of $\tilde{x}_2$ towards 0.

From (5.40), the convergence of the errors $\dot{\tilde{x}}_3$toward 0 is then ensured. We also show that the estimation error of the longitudinal forces is bounded.

In the following paragraph, we give some experimental results to show the quality of the proposed observer.

5.4.2 Experimental Results

In this section, we give some results in order to test and validate our approach. The estimated road profile is compared to the profile measured by an longitudinal profile analyzer (LPA) developed at the LCPC Laboratory [LDG96]. It is equipped with a laser sensor and an accelerometer to measure the elevation of the road profile as shown in the Fig. 5.8.

Fig. 5.8 Longitudinal Profile Analyzer (APL in french)

The model parameters are measured. However, the pneumatic parameters C_1, C_2 and C_3 are not well known. To mitigate this disadvantage, we use observers to estimate the longitudinal forces which are related to these parameters. The system outputs are the displacements of the wheels and the chassis, which correspond to the signals given by the sensors. Different measurements are done with the vehicle moving at several speeds.

Fig. 5.9 shows the average vehicle speed of $70km/h$ ($20m/s$) with an error which does not exceed $1.2m/s$.

This figure shows the measured and the estimated displacements. In the first two subplot on top of figure (5.10), the vertical displacement (z) and the yaw angle (ψ) of the chassis respectively are presented.

It is shown that the estimation of these displacements is fast and of good quality.

The bottom of this figure represent the velocities. We can see that the estimated vertical velocity ($\dot{z}$) is accurate compared to the true signal.

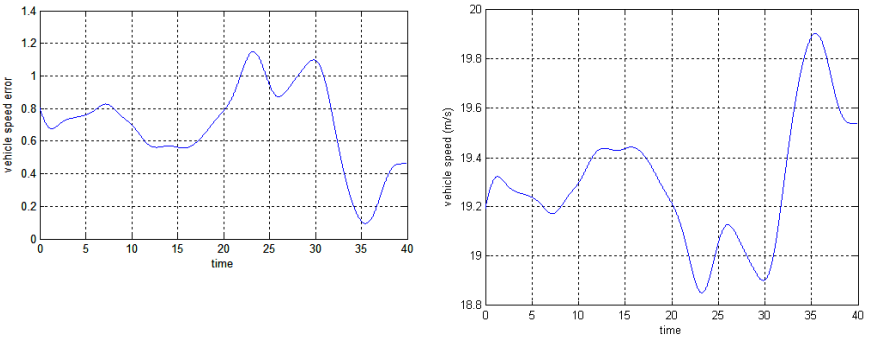

Fig. 5.9 Vehicle speed

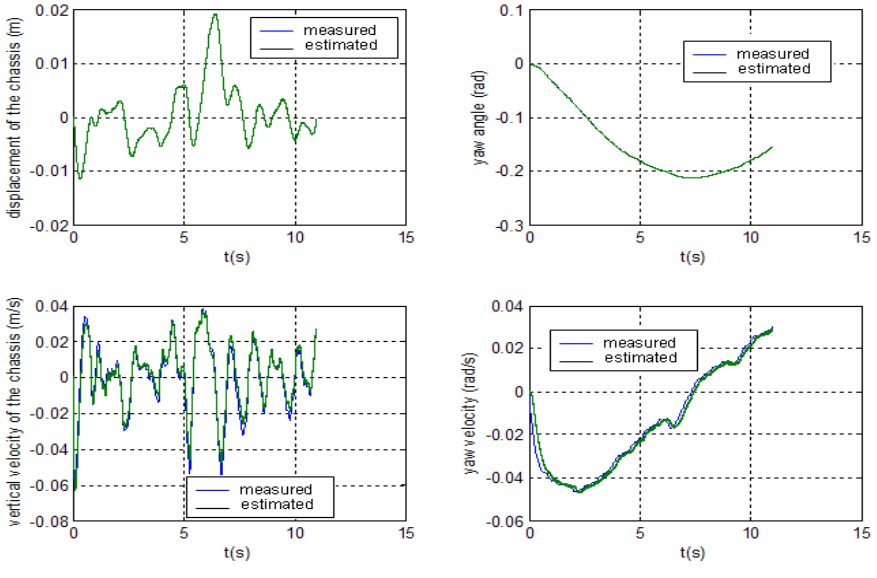

Fig. 5.10 Estimated and measured states: chassis and yaw angle

However, some error occurs concerning the estimation of $\dot{\psi}$. This error is mainly due to sensor calibration (the sensor that we used in our measurement presented an error of calibration that we could not correct).

In Fig. 5.11 we notice that the estimated angular velocity of the wheel converges well towards the actual ones in finite time.

Indeed, we get only 1 *second* for the convergence time.

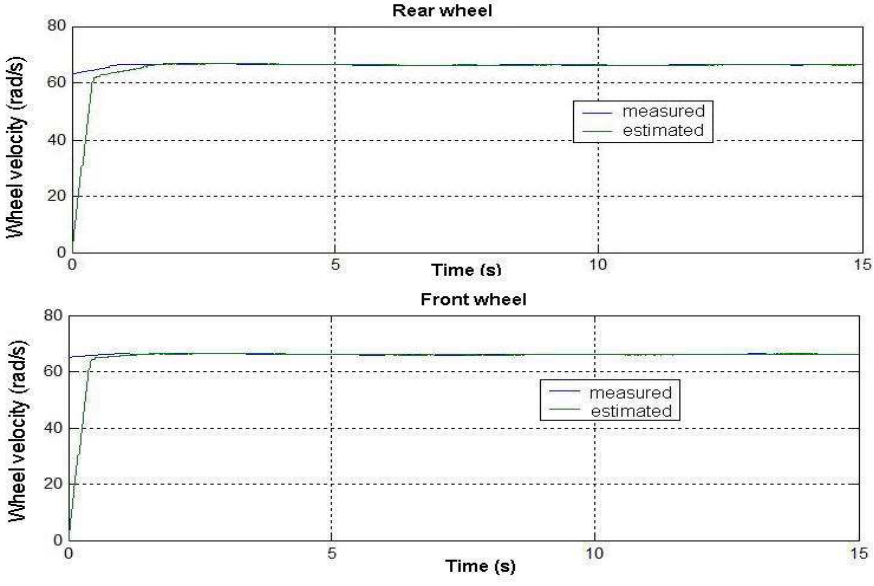

Fig. 5.11 Estimated and measured wheels velocities

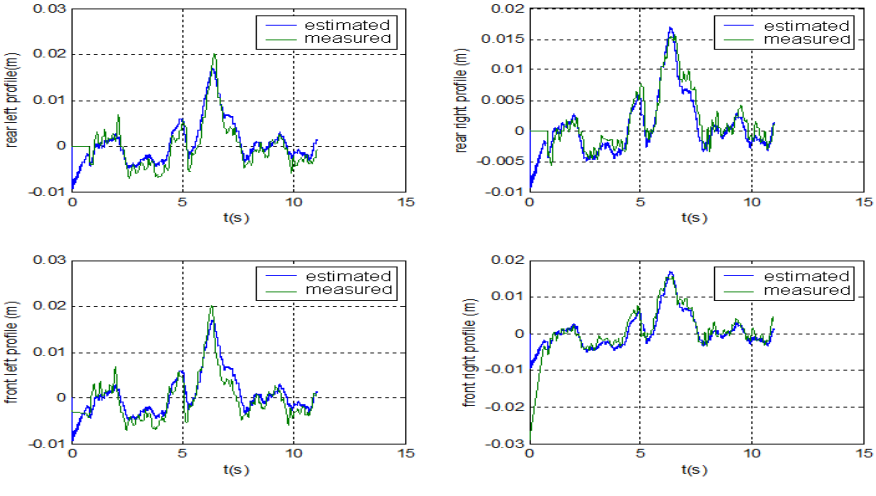

Fig. 5.12 Comparison between the LPA measured profile and estimated one

The convergence of the states is very fast and the estimation is of high quality. The good reconstruction of these states allows estimating the unknown inputs.

In Fig. 5.12 we show the behavior of the road profile estimator.

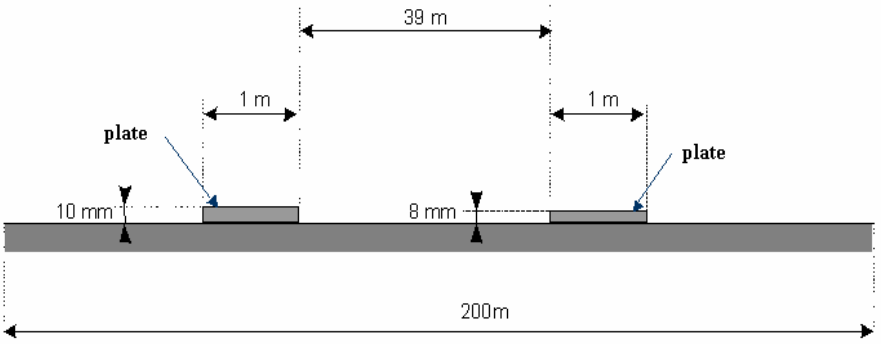

Fig. 5.13 Postions of the plates on the track

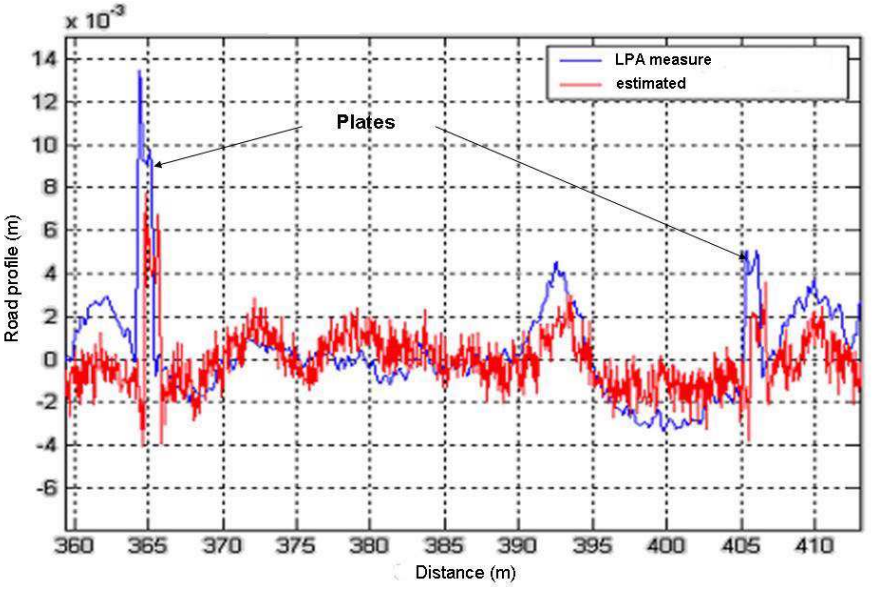

Fig. 5.14 Plates estimation

This figure presents both the measured road profile and the estimated one.

As a further example, two plates are located on the track as shown in Fig.5.13.

Fig. 5.14, shows that these plates of height, respectively, of $10mm$ and $8mm$, are well reconstructed by the observers approach compared to the LPA measurements.

We compare now, the results of each method developed earlier.

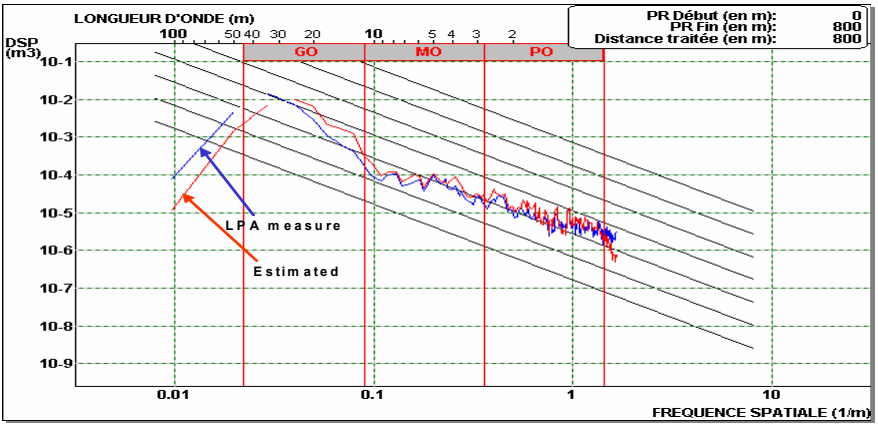

Fig. 5.15 Power Spectral Density (PO: low wave, MO: average wave, GO: high wave

One can then observe that the estimated values are quite close to the true ones. These profiles have the same pace and the differences are not important.

Fig. 5.15 shows the power spectral density of the estimated road profile and the measured one given by LPA instrument.

One notices that the low and average waves of the road (high and average frequency) are well reconstructed. However there are limitations of our method to estimate the high waves of the road.

5.5 Conclusion

In this chapter sliding mode observers have been developed in order to estimate the longitudinal tire/road forces of the system and the unknown inputs which correspond to the road profile.

The parameters of the system are presumedly measured and known. However, the pneumatic coefficients which intervene in the calculation of the longitudinal forces are unknown. This is why we built another observer to directly consider these longitudinal forces. We noticed that the profile estimated by our approach is very close to that measured by the LPA instrument. However, local variations appear. It is then important to know if these variations do not penalize the capability of these profiles (of a band-width broader than APL) to determine the dynamic response of the vehicle (previous studies have shown that in the profile measured by LPA, it is not correct to consider this dynamic response). We consider, in the future work, these profiles as inputs of a dynamic model of the vehicle to estimate the instantaneous loads of the wheels. We thus compare the dynamic responses measured on an instrumented vehicle and those estimated by the simulator of the vehicle.